Model for fusion and cool compound nucleus formation based on the fragmentation theory

Neelam Malhotra, R. Aroumougame, and D. R. Saroha
Physics Department, Panjab University, Chandigarh-160014, India

Raj K. Gupta*
International Centre for Theoretical Physics, Trieste, Italy
and Physics Department, Panjab University, Chandigarh-160014, India
(Received 12 August 1985)

Collective potential energy surfaces are calculated in both the adiabatic and sudden approximations by using the asymmetric two-center shell model in the Strutinsky method. It is shown that fusion of two colliding heavy ions occurs by their crossing over of the adiabatic interaction barrier. The adiabatic scattering potentials present two barriers, whereas no barrier is shown to occur in sudden scattering potentials. The first barrier is obtained just past the saddle shape but is too low, such that a deep inelastic process is expected. The other, inner, barrier is high enough to let the system fall into the fusion well, whose excitation energy then determines whether a cool compound nucleus is produced or the fusion-fission process occurs. For a given compound nucleus, the excitation energy is found to be small for only a few target-projectile combinations, which increase as their mass asymmetry increases. Such target-projectile combinations which refer to a cool compound nucleus can be identified by a simple calculation of the fragmentation potential based on the ground state binding energies with Coulomb and proximity effects calculated at a constant relative separation of the two nuclei. Our calculations are made for the composite systems with $102 \leq Z \leq 114$.

I. INTRODUCTION

The question, "How do colliding nuclei fuse and then why and when does the compound system formed go to the ground state and give a stable compound nucleus or fission instead?" has always been of much theoretical interest.[1-5] The importance of such a question has become more apparent due to some recent experiments: whereas collisions at one bombarding energy (e.g., 265 and 280 MeV ^{208}Pb on ^{50}Ti and ^{52}Cr, respectively[6,7]) lead to measurable fusion cross sections, for the same target and projectile (and many others) at another energy[8] (4.8–8 MeV/nucleon ^{208}Pb on different targets of ^{26}Mg, ^{48}Ca, ^{50}Ti, ^{52}Cr, ^{58}Fe, and ^{64}Ni), the fusion excitation functions as well as the symmetric mass fragmentations of the compound systems are measured. According to Swiatecki,[5] the fused systems obtained in these reactions of ^{208}Pb on various targets[8] could either be true compound nuclei trapped inside the true saddle or simply the composite nuclei (also called mononuclei) trapped inside some conditional saddle.

In this paper, we show that within the fragmentation theory based on the two-center shell model, the fusion of colliding nuclei occurs by overcoming an adiabatic interaction barrier. Fusion starts already at the first outer barrier, located past the saddle shape formation. There is, however, a second inner barrier that must be overcome for achieving the complete fusion. This essentially constitutes our model for the fusion of two nuclei. The excitation energy of the compound system so formed is given by the height of the inner barrier, and this along with the corresponding nuclear shapes determine the exit channel effects; i.e., whether it proceeds to form a cool compound nucleus after the evaporation of a few neutrons or gives rise to the process of "fusion-fission." A cool compound nucleus means the compound nucleus with a minimum of excitation energy, for which the number of neutrons evaporated is small and consequently the cross section for its formation in the ground state is large. On the other hand, for the system to fission in the exit channel, it must be strongly excited and the nuclear shapes must have neck formations after the saddle is formed. In case the incident energy is not enough for the system to cross over the inner barrier, then because of the outer barrier (which is only a small bump), damped or deep inelastic collision (also, called "quasifission") occurs since a (conditional) saddle is shown to be formed here.

The method for calculating the adiabatic and sudden interaction potentials, using the fragmentation theory, is described briefly in Sec. II. The fusion model based on these potentials is then given in Sec. III. A relative comparison of the fusion excitation energies, i.e., the adiabatic barrier heights, for different target-projectile combinations forming the same compound system, is carried out in Sec. IV which allows us to optimize the choice of target-projectile combinations corresponding to the cool compound nuclei. The calculations are made for collisions of any two nuclei with masses larger than 40 u, forming compound systems with $102 \leq Z \leq 114$. A summary of our results is given in Sec. V and an application of this model to the data[8] of symmetric mass fragmentation following capture is made in a subsequent paper[9] (hereafter referred to as II).

II. METHOD FOR CALCULATING THE POTENTIAL ENERGY SURFACES

The fragmentation theory introduces[10,11] two new collective coordinates of mass — and charge — asymmetries, respectively,

$$\eta=(A_1-A_2)/(A_1+A_2) \tag{1a}$$

and

$$\eta_Z=(Z_1-Z_2)/(Z_1+Z_2), \tag{1b}$$

in the nuclear shape which is taken to be described by the asymmetric two-center shell model (ATCSM).[12] Here $A=A_1+A_2$ and $Z=Z_1+Z_2$, with A_i and Z_i $(i=1,2)$ referring to incoming nuclei or outgoing fragments. These two coordinates are, of course, in addition to the other commonly used coordinates of: (*i*) relative separation R or equivalently, the length parameter $\lambda=l/2R_0$, with l the length of the nucleus and R_0 the radius of the corresponding spherical nucleus; (*ii*) the deformation coordinates β_1 and β_2, defined as the ratios of major to minor axes; and (*iii*) the neck parameter ϵ, giving the ratio of the actual barrier to the rounded-off barrier between two harmonic oscillator potentials.

The collective Hamiltonian is then of the form

$$H=T(\mathbf{R},\beta_i,\eta,\eta_Z;\dot{\mathbf{R}},\dot{\beta}_i,\dot{\eta},\dot{\eta}_Z)+V(\mathbf{R},\beta_i,\eta,\eta_Z)\ , \tag{2}$$

where the collective potential V is obtained in the Strutinsky way[13] by renormalizing the sum of single-particle states of the ATCSM to an appropriate liquid drop model (LDM).[14] Depending on whether the collision proceeds adiabatically or as a sudden process, in the ATCSM the instantaneous oscillator frequency $\omega(R)$ at the separation distance R is, respectively, the frequency $\omega_v(R)$ for which the volume enclosed by an equipotential at the surface is conserved, or ω_∞, the same frequency the colliding nuclei had when they were far apart at infinity. In other words, the oscillator frequency in the case of sudden collisions is fixed and equal to its asymptotic value ω_∞ for all relative separations R. For sudden collisions, the liquid drop energy also contains an additional term[15] due to the compression effect, since the relative velocities of the colliding nuclei are now assumed to be high. We fix the shape parameters β_1, β_2, and ϵ by minimizing the potential V in these coordinates for the adiabatic approximation, and by taking the ground state deformations β_1 and β_2 of the incoming nuclei with $\epsilon=1$ for the sudden collisions.

For the asymptotic limit, i.e., $R>R_1+R_2$, the potential is defined simply as

$$V(R,\eta)=-B_1(A_1,Z_1)-B_2(A_2,Z_2)+E_C+V_p+V_l\ , \tag{3}$$

where $B_i(A_i,Z_i)$ are the experimental nuclear binding energies (taken from the tables of Seeger[16] which are calculated for the liquid drop energy smoothed with shell corrections from the Nilsson model), minimized in the η_z coordinate, and E_C, V_p, and V_l are, respectively, the Coulomb interaction energy, the proximity nuclear potential, and the rotational energy due to angular momentum l. In this paper, however, we limit ourselves to the $l=0$ case, i.e., $V_l=0$. For the Coulomb interaction, though various prescriptions are available,[17–19] we use here the expression of Aroumougame and Gupta,[3] obtained by following Hirschfelder *et al.*[20] and Nix[21] (see also Webster[22]), for two arbitrarily oriented prolate spheroids separated by a distance $R>R_1+R_2$. Their expression simplifies to the usual form

$$E_C=\frac{Z_1Z_2e^2}{R} \tag{4}$$

for spherical nuclei. The proximity potential between two spherical nuclei is given by the "pocket formula" of Blocki *et al.*,[23]

$$V_p=4\pi\gamma b\bar{R}\Phi(\zeta_0)\ , \tag{5a}$$

where $\zeta_0=s_0/b$, with the separation distance $s_0=R-R_1-R_2$;

$$\bar{R}=R_1R_2/(R_1+R_2)\ , \tag{5b}$$

$$R_i=1.28A_i^{1/3}-0.76+0.8A_i^{-1/3}\approx 1.15A_i^{1/3}\quad (i=1,2)\ , \tag{5c}$$

$$b\approx 1\text{ fm}\ , \tag{5d}$$

$$\gamma=0.9517\left[1-1.7826\left[\frac{N-Z}{A}\right]^2\right]\text{ MeV/fm}^2\ , \tag{5e}$$

and the dimensionless universal function

$$\Phi(\zeta_0)=-\tfrac{1}{2}(\zeta_0-2.54)^2-0.0852(\zeta_0-2.54)^3\quad \zeta_0\le 1.2511$$
$$=-3.437\exp(-\zeta_0/0.75)\quad \zeta_0\ge 1.2511\ . \tag{5f}$$

This function is defined for negative (overlap region), zero (touching configuration), and positive values of s_0, although for negative s_0 the definition becomes somewhat arbitrary (see Refs. 24 and 25 and the Appendix for further discussion on this point). The possible generalization of (5) to deformed and oriented nuclei is presented in the Appendix, which is worked out in the central line prescription[26] because of its computational simplicity. Realistic derivations of the proximity potential for collision of two coplanar, deformed, and oriented nuclei are given in Refs. 24, 25, and 27.

III. FUSION MODEL—ADIABATIC AND SUDDEN INTERACTION POTENTIALS

The necessary condition for the fusion of two colliding nuclei is the occurrence of a potential barrier (also called the "interaction barrier" or the "fusion barrier") after the saddle is formed, or the presence of a deep "pocket" in the interaction potential. The interaction barrier is shown[2,28] to lie higher and at a much smaller value of R than the Coulomb barrier. The presence of an interaction barrier is interpreted[2] to mean that during collisions the nuclei would arrive at the top of the barrier (called the point of no return) and fall into deep "fusion well" behind the barrier, stick together due to loss of enough kinetic energy, and form a compound nucleus. Then, depending on its excitation energy, the compound nucleus would either go to the ground state by emitting a couple of neutrons or ex-

hibit some other phenomenon, like the preformation of fission fragments (the fusion-fission), etc. Since a compound nucleus can be reached by various combinations of the targets and projectiles and collisions can occur both adiabatically or as a sudden process, it is of interest to study the interaction potentials calculated under both the adiabatic and sudden approximations and for various target-projectile combinations referring to the same compound nucleus. This is done in the following, and a relative comparison of the excitation energies of the compound nucleus formed through different target-projectile combinations is carried out in Sec. IV.

Figure 1 shows our calculated adiabatic and sudden scattering potentials $V(\lambda)$ for a number of different target-projectile combinations (η values) forming the same compound nucleus $^{258}104$. The potentials in two approximations are matched at the touching configurations ($\lambda \approx 1.5$) for the sudden case. For $\lambda > 1.5$, the sudden potentials are shown to be lower due to Coulomb effects, whereas at this length the adiabatic potentials still show the presence of nuclear effects that are known to be predominant up to a separation distance of ~ 1.7 fm (Ref. 28). The corresponding nuclear shapes are given in Fig. 2.

We notice in Fig. 1 that for adiabatic collisions, the interaction or fusion barriers (marked λ_F) are obtained for all the target-projectile combinations having $\eta \leq 0.5$. This

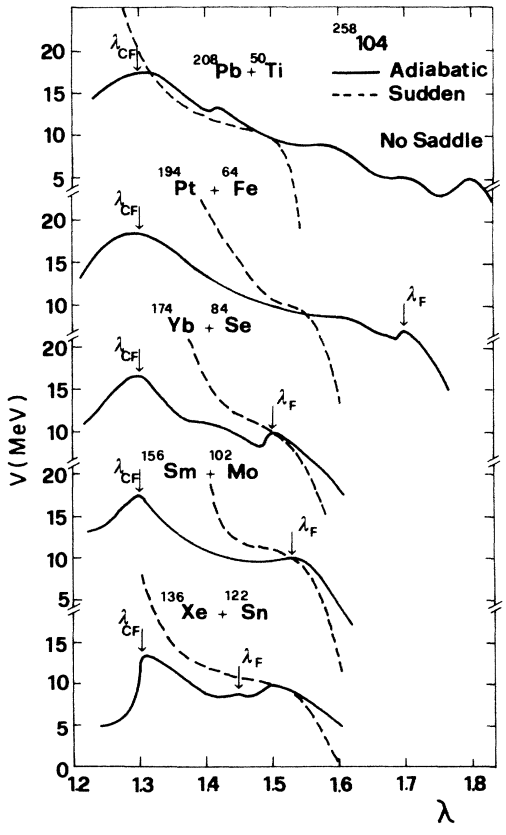

FIG. 1. The adiabatic and sudden scattering potentials for various target-projectile combinations forming the compound system $^{258}104$. The two sets of graphs are matched at the touching configurations ($\lambda \approx 1.5$) for sudden collisions. The positions of the two barriers in the adiabatic case are also indicated.

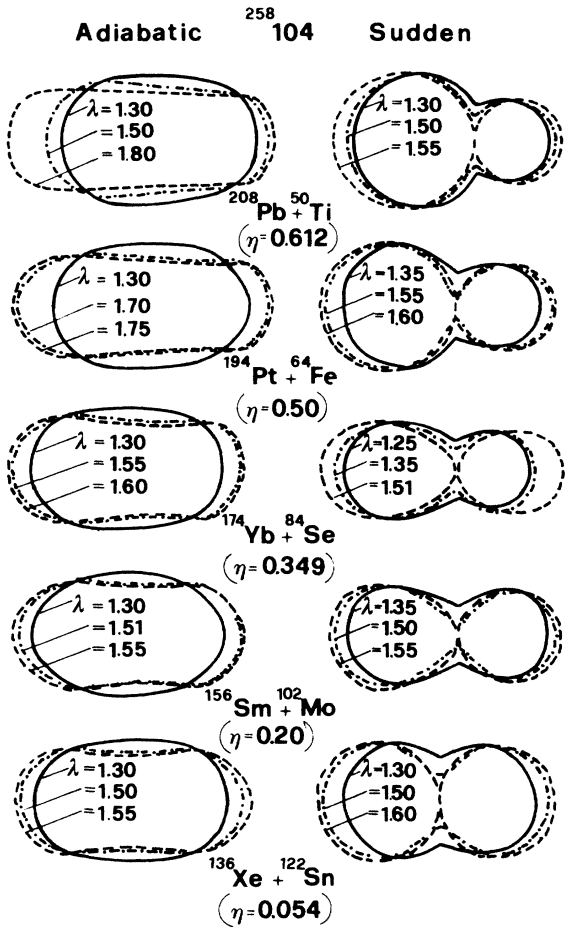

FIG. 2. The nuclear shapes in both the adiabatic and sudden approximations at different lengths (λ values) for the target-projectile combinations of $^{258}104$ considered in Fig. 1.

barrier occurs at a point just after the saddle shape is formed (see Fig. 2). For $\eta > 0.5$, the saddle shape is not formed (see the case of ^{208}Pb + ^{50}Ti, $\eta = 0.612$, in Fig. 2) although the interaction barrier is still seen in Fig. 1 at a somewhat larger λ value ($\lambda \approx 1.8$). The occurrence of an interaction barrier past the saddle shape means that the colliding nuclei start to fuse already at this length of the compound system, called the "fusion length" λ_F. However, this barrier is obtained only as a small bump and will not be able to hold the colliding system together. In other words, at this energy the saddle formed at λ_F is a kind of "conditional saddle"[5] leading to "quasifission" or "deep-inelastic collision" of the intermediate compound system (the mononucleus) formed. In Fig. 1, however, there is a second barrier (marked λ_{CF}), that is shown in each case at a much shorter length of the compound nucleus, called the "complete fusion length" λ_{CF}. This barrier is apparently high, so that if the colliding nuclei cross over it, they will fall into the deep "fusion well" behind it and may proceed to form a stable compound nucleus. An additional incident energy is clearly required for this process of complete fusion to happen.

On the other hand, for sudden collisions we notice in

Fig. 1 that no interaction barriers or deep pockets appear in the scattering potentials, though the nuclear shapes in Fig. 2 show neck and saddle formations. The neck is, however, known to develop suddenly from $\epsilon \geq 1$ in the entrance (or fusion) channel to $\epsilon \approx 0$ in the exit (or fission) channel with a gain of about 40 MeV energy (see Fig. 6.7 in Ref. 29). This means that even if the colliding nuclei at infinity approach in a sudden approximation, once they touch, the neck formed gets filled quickly and the collision proceeds adiabatically. In any case, at low incident energies of 5—10 MeV/nucleon, the collisions are not expected to proceed via sudden approximation, except for the nuclear molecule formation. Also, there are other macroscopic slowing-down forces of friction and viscosity which increase the collision time and make it more favorable for the collision process to be adiabatic.

We have also made calculations of adiabatic and sudden scattering potentials for a number of other target-projectile combinations forming compound nuclei with $102 \leq Z \leq 110$. This is shown in Fig. 3, only for nearly symmetric ($\eta \approx 0$) and asymmetric ($\eta > 0.5$) combinations. We notice that exactly the same results as obtained above for $^{258}104$ are given.

Summarizing, our "fusion model" involves the following steps: We calculate the adiabatic scattering potentials for all the possible target-projectile combinations of a given compound nucleus. The nuclear shape in this approximation is fixed by minimizing the potential energy in deformations and neck coordinates. In this way, the saddle shape and the interaction barriers are located. The fusion of the colliding nuclei starts already at the first outer barrier, but deep-inelastic collision takes place since this barrier is not high enough to hold the system together. Allowing for dynamical distortion effects and the role of classical friction and viscosity, if the incident energy is large enough to come up to the top of the second inner barrier, the colliding nuclei would fall into the deep "fusion well" and stick together due to loss of enough kinetic energy. This compound system will then either go to the ground state by emitting a few neutrons, or manifest the preformation of fission fragments, etc., depending on its excitation energy.

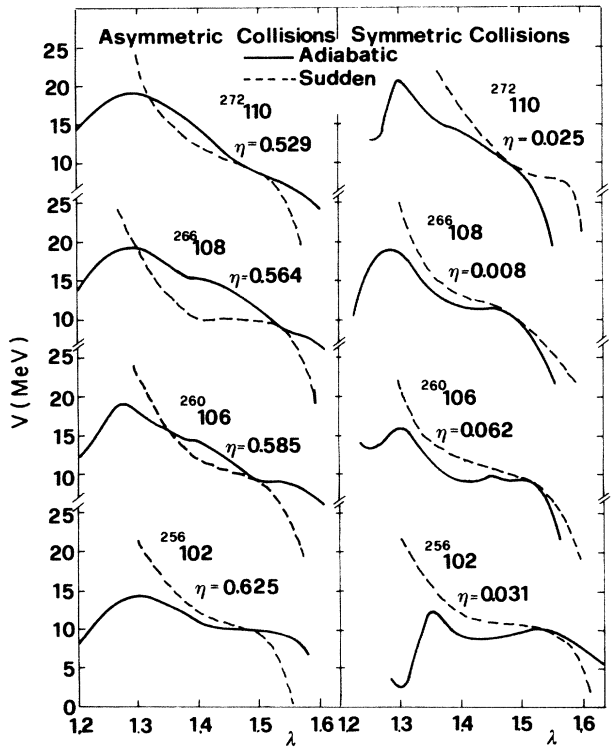

FIG. 3. The adiabatic and sudden scattering potentials for the (nearly) symmetric and asymmetric target-projectile combinations forming the compound systems $^{256}102$, $^{260}106$, $^{266}108$, and $^{272}110$.

IV. THE FUSION MODEL AND THE COOL COMPOUND NUCLEUS FORMATION

The excitation energy of the compound system is given by the height of the interaction barrier, which is apparently different for different target-projectile combinations (η values) used. Then a plot of these barrier heights as a function of mass asymmetry η gives the so-called fragmentation potential $V(\eta)$. Notice that here the length of the nucleus λ (or the R value) for each η value corresponds to the point at which the fusion actually occurs. This is important because in all our earlier calculations of fragmentation potentials (see, e.g., Refs. 1—4), we made an approximation of using a constant value of R in order to save the large computer time involved in the three-dimensional minimization of the potential energy surfaces. For the same reason, we determine here the dependence of barrier positions λ_F and λ_{CF} on η from a few carefully calculated points, rather than calculating the scattering potentials for all possible target-projectile combinations of a compound system, as is required by our fusion model. This is done in Fig. 4 for $^{258}104$ by using

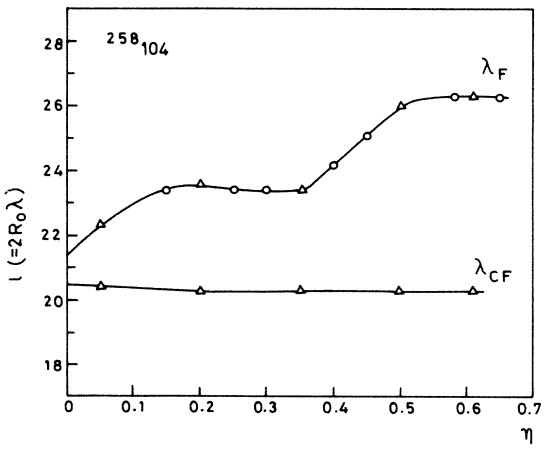

FIG. 4. Variations of the "fusion" length λ_F and the "complete fusion" length λ_{CF} with mass asymmetry η for the compound system $^{258}104$. The triangles refer to the scattering potentials in Fig. 1 and the open circles are for the other intermediate points for which λ_F was determined by calculating the relevant parts of the scattering potentials.

the adiabatic scattering potentials of Fig. 1. In addition to the five points from Fig. 1 (shown as triangles), the λ_F barriers for a few other intermediate η values were also calculated, which are shown here as open circles. (The full scattering potentials were not calculated for these intermediate points.) For $\eta=0.612$ (^{208}Pb + ^{50}Ti), although no saddle shape was obtained, we have taken the barrier at $\lambda_F=1.80$ and extrapolated the λ_F curve smoothly up to $\eta=0.65$. Beyond this η value, the two-center shell model does not remain very reliable since one of the colliding nuclei is then a light nucleus.

We notice from Fig. 4 that the barrier position at λ_{CF} is almost independent of η, whereas $\lambda_F(\eta)$ shows a steplike functional increase. Using these lengths (rather than constant values[1-4]), the fragmentation potentials $V(\eta)$ are calculated for both cases. These are plotted in Fig. 5, marked λ_F and λ_{CF}. For comparison, we have also plotted here the fragmentation potential for a constant value of $R=14.2$ fm, calculated by using Eq. (3). We observe that the basic structure of the two potential energy surfaces, obtained by calculating the true fusion barriers (curves marked λ_F and λ_{CF}), is identical and is comparable with that for the fragmentation potential calculated simply at a constant $R=14.2$ fm. In particular, all the potential energy minima are nearly at the same η values, and the variations of their excitation energy with respect to η are identical. We are interested only in the potential energy minima, since at the minimum $\partial V/\partial\eta=0$, and according to Săndulescu *et al.*[1], for headon collisions, the compound nucleus reached through such target-projectile combinations would be very much cooler compared to that formed by reaction partners belonging to an η value lying outside the minima. For η values away from the minima, the driving force $-\partial V/\partial\eta$, according to classical mechanics, is nonzero, which will make the system run in the direction of the potential minima, accompanied by a large mass transfer and hence transfer of energy into the excitation of surface vibrations.

Hence, from Fig. 5, we have obtained two important results: (i) the idea of using constant R ($>R_1+R_2$) in our earlier calculations[1-4] of the fragmentation potentials is quite reasonable for locating the target-projectile combinations that form cool compound nuclei; (ii) the mass asymmetry degree of freedom η plays an important role in determining the excitation energy of these cool com-

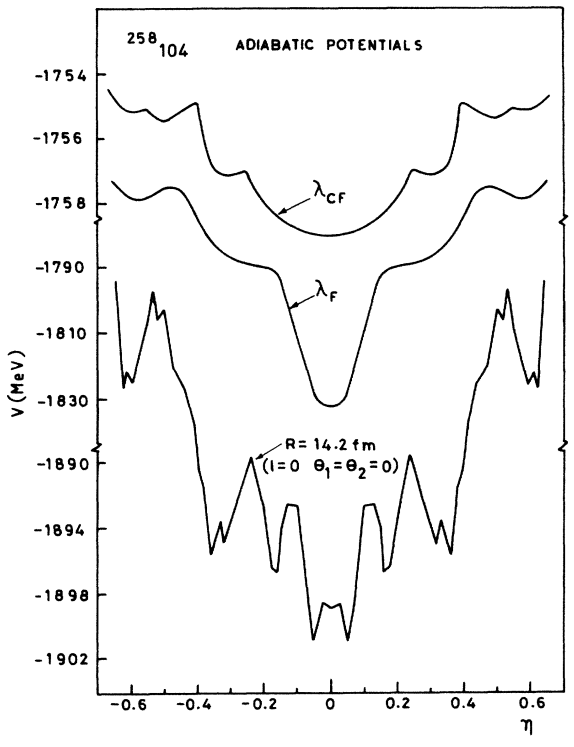

FIG. 5. The adiabatic fragmentation potentials for ^{258}104, calculated for the constant relative separation $R=14.2$ fm [using the ground state binding energies from Seeger (Ref. 16)] and for the lengths $\lambda_F(\eta)$ and $\lambda_{CF}(\eta)$ given in Fig. 4. The proximity contribution is added for the cases of constant R and $\lambda_F(\eta)$ by using Eq. (5) and the method described in the Appendix.

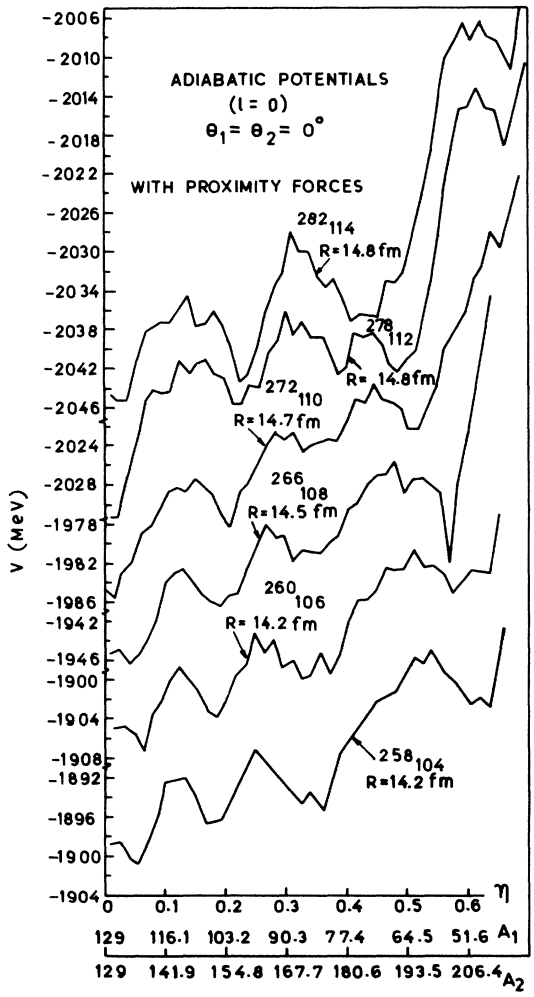

FIG. 6. The adiabatic fragmentation potentials for various compound systems with $104\leq Z\leq 114$, calculated at constant R values by using the ground state binding energies of the colliding partners [taken from Seeger (Ref. 16)] with the Coulomb and proximity potentials added to it.

pound nuclei. The excitation energy increases as η increases. Specifically, the compound nucleus formed due to an asymmetric target-projectile combination is very much excited compared to that formed through symmetric or nearly symmetric reaction partners. As a test of this result, we apply our model in II to the data of Bock *et al.*[8] We show that the measured capture cross sections as a function of incident energy are reasonably reproduced by letting the incoming nuclei be captured by the inner adiabatic interaction barrier and that, because of the large mass asymmetry of the incoming nuclei, the captured (or fused) system fissions back with symmetric mass distribution, in satisfactory agreement with experiments.

Finally, we have used the first result of our last paragraph for calculating the fragmentation potentials $V(\eta)$ at constant R values. This is done for a number of compound systems with $106 \leq Z \leq 114$, and the calculated fragmentation potentials are shown in Fig. 6. The potential for $^{258}104$ is also reproduced for completeness. The interesting result from Fig. 6 is that in all cases, only four or five target-projectile combinations are shown to give the compound nuclei with small excitation energies (i.e., the cool compound nuclei), and once again the excitation energies of these cool compound systems increase with the mass asymmetry of their reaction partners.

V. SUMMARY OF THE RESULTS

We have shown that, on the basis of fragmentation theory which uses the two-center shell model, fusion of two heavy ions can take place only if they overcome the adiabatic interaction barrier. Actually, the fusion process starts already at the first barrier which appears at a much larger length (or separation) of the colliding system, at a point just past the saddle shape formation. This barrier is, however, too low such that only a "conditional saddle" can be said to be formed and the deep-inelastic collision process occurs. Another barrier at a smaller length of the composite nucleus is also observed which is high enough to hold the system together. Provided the incident energy is good enough, complete fusion of the colliding nuclei occurs by crossing over of this barrier. Then, depending on the excitation energy of the fused system formed (given by the barrier height), it will either go to the ground state after evaporating a few neutrons (producing a compound nucleus) or fission back, resulting in a fusion-fission process.

The excitation energies, i.e., the fusion barrier heights, calculated for all the possible target-projectile combinations of a compound nucleus, when plotted as a function of their mass asymmetry, give the fragmentation potential. This calculation, upon comparison with the fragmentation potential calculated simply for a constant relative separation (larger than the sum of radii of the incoming nuclei), gives two further interesting results: (i) the use of a constant value of relative separation in the calculations of the fragmentation potential is a reasonable approximation for locating the target-projectile combinations corresponding to cool compound systems; (ii) the excitation energies of the cool compound system increase as the mass asymmetry of the incoming nuclei increases.

ACKNOWLEDGMENTS

This work was supported by the University Grants Commission, New Delhi and the Department of Atomic Energy, Government of India. One of us (R. K. G.) is grateful to Professor Abdus Salam, the International Atomic Energy Agency, and UNESCO for the hospitality at the International Centre for Theoretical Physics, Trieste.

APPENDIX: PROXIMITY POTENTIAL FOR DEFORMED, ORIENTED COLLISIONS WITHIN THE CENTRAL LINE PRESCRIPTION

The central line prescription consists in calculating the proximity potential with the distance s_0 between the nuclear surfaces as the one along the line connecting the nuclear centers (the central line) rather than the shortest distance between them. Also, the variation of the mean curvature radius $\bar{R}$ with the angle of orientation of the surface is neglected. Such an approach has been quite successful for light ions. For a heavy spherical projectile on a heavy deformed nucleus, however, Randrup and Vaagen[26] have shown that this prescription gives the potential to within 10% only if surfaces with quadrupole deformations are considered. More recently, Baltz and Bayman[27] have also shown the inadequacy of the "central line potential" within the proximity approach, if either of the nuclear surfaces has high multipole (hexadecapole) deformations. In spite of all its inadequacy, it is still very much used because of its being computationally very simple. In the following, we use it for the collision of two deformed, oriented nuclei having quadrupole deformations. Our treatment is somewhat similar to that of Tricoire *et al.*,[30] who studied the deformation effects in the proximity potential for two axially aligned nuclei ($\theta_1=\theta_2=0$ in Fig. 7).

For spherical nuclei, the proximity potential is adequately given by Eqs. (5). When both the colliding nuclei are deformed, the surface separation in the central line prescription for the axially symmetric nuclei lying in the same plane is given by

$$s_0 = R - R_1 - R_2 \ , \tag{A1}$$

where the nuclear radii are now defined by

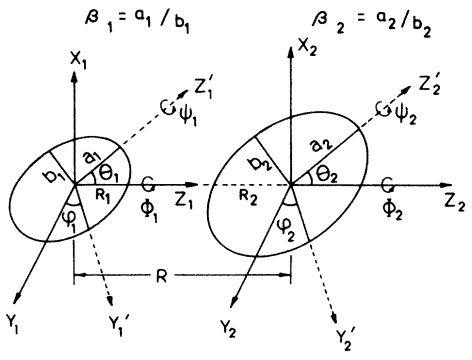

FIG. 7. A schematic configuration of two deformed and oriented colliding nuclei.

$$R_i(\theta_i)=R_i[1+\alpha_i P_2(\cos\theta_i)] \quad (i=1,2) . \tag{A2}$$

Here θ_i is the angle of rotation of the ith nucleus with respect to the symmetry axis (see Fig. 7) and α_i are related to the quadrupole deformation β_i (see Ref. 16 for a definition of α_i),

$$\beta_i=1+1.5\alpha_i+1.6\alpha_i^2+\text{higher orders} . \tag{A3}$$

R_i is given by Eq. (5c), but in the actual calculations we use the central radii C_i instead of these effective sharp radii, where[23]

$$C_i=R_i-\frac{b^2}{R_i} . \tag{A4}$$

We use definition (A1) for only the positive s_0, i.e., for $R\geq R_1+R_2$. For negative s_0, this definition becomes quite arbitrary[24,25] and we use an alternative definition given below.

The mean curvature radius $\overline{R}$ for two deformed nuclei is given by[23]

$$\frac{1}{\overline{R}^2}=\frac{1}{R_{11}R_{12}}+\frac{1}{R_{21}R_{22}}+\left[\frac{1}{R_{11}R_{21}}+\frac{1}{R_{12}R_{22}}\right]\sin^2\varphi + \left[\frac{1}{R_{11}R_{22}}+\frac{1}{R_{21}R_{12}}\right]\cos^2\varphi , \tag{A5}$$

where φ is the azimuthal angle between the principal planes of curvature of nucleus 1 and 2; and R_{ii} are the four principal radii of curvature, at the points of minimum separation (see Ref. 27 for explicit expressions). For coplanar nuclei, $\varphi=\varphi_1-\varphi_2=0°$, and if the two nuclei have their symmetry axes aligned with the collision axis, i.e., $\theta_1=\theta_2=\theta=0°$ (as is the case for the calculations of Figs. 5 and 6), then (A5) reduces to

$$\frac{1}{\overline{R}^2}=\frac{1}{a_1a_2}+\frac{1}{b_1b_2}+\frac{1}{a_1b_2}+\frac{1}{a_2b_1} , \tag{A6}$$

where a_i and b_i are the semimajor and semiminor axes of the two colliding deformed nuclei (Fig. 7).

For the nuclear surface width b and the surface energy coefficient γ, we take the values given by Eqs. (5d) and (5e), respectively. Tricoire *et al.*[30] allow for the deformation effects in b as well.

In the case of the interaction region, i.e., $R<R_1+R_2$, the saddle and necked shapes are formed. The proximity potential would then apparently depend on the shape parameters also, as is shown in Ref. 25 for two equal colliding nuclei. For the present calculations, however, we still use Eqs. (5) with s_0 defined as the difference between the length of the nuclear system obtained by minimizing the liquid drop energy (see Fig. 2, adiabatic case, for typical shapes) and the corresponding length of the colliding partners at their touching configuration,

$$s_0=2R_0\lambda-2(R_1+R_2) . \tag{A7}$$

Apparently, now s_0 can be both positive and negative and the proximity term contributes till the neck disappears. $\overline{R}$ is still given by Eq. (A6).

A proper derivation of the proximity potential for the collision of two coplanar, axially symmetric deformed and oriented nuclei is given by two of us[25] and it will be of interest to compare the present central line prescription results for deformed nuclei with the corresponding realistic calculation. As already mentioned in the first paragraph of this Appendix, Randrup and Vaagen[26] have carried out such a comparison for a spherical-plus-deformed system. However, instead of carrying out such a comparison here, in the following we look for the justification of the above approach by analyzing its role in the heavy-ion fragmentation potentials. Calculations are made for both the asymptotic ($R\geq R_1+R_2$) and interaction ($R<R_1+R_2$) regions.

First of all, we study the variation of the proximity potential V_p as a function of mass asymmetry η and the orientation θ_1 and θ_2 of the colliding nuclei. We consider the case of $R\geq R_1+R_2$ and $\theta_1=\theta_2=\theta$. Figures 8 and 9 show the results of our calculation for the compound system $^{258}104$ as an illustrative example. We notice in Fig. 8(a) that the proximity contribution is small for large surface separations (see the dashed line for $R=15$ fm, plotted for the case of $\theta=0°$ only). As R is decreased to 14.2 fm, the proximity potential is still negligibly small, almost

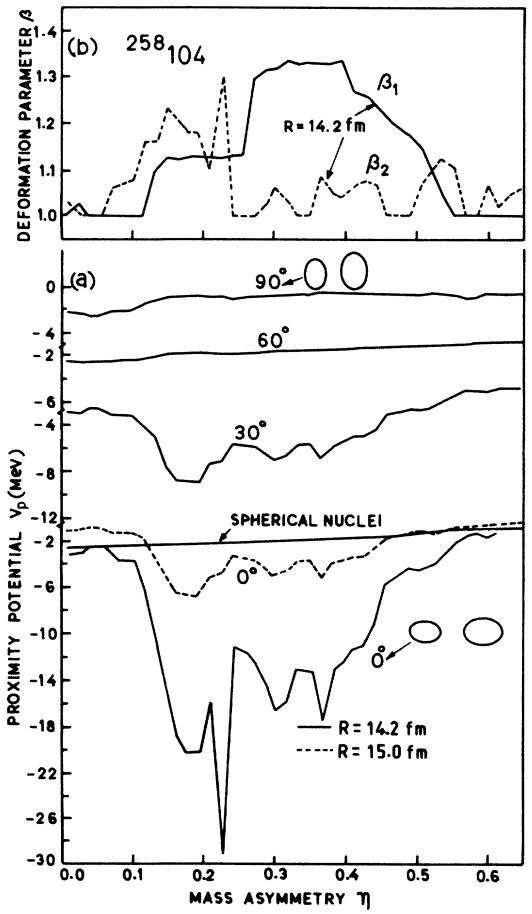

FIG. 8. (a) The proximity potential as a function of mass asymmetry, within the central line prescription, for the compound system $^{258}104$ at constant R values ($>R_1+R_2$) and at different orientations $\theta_1=\theta_2=\theta$. (b) The deformations of the two colliding nuclei as a function of mass asymmetry for $^{258}104$.

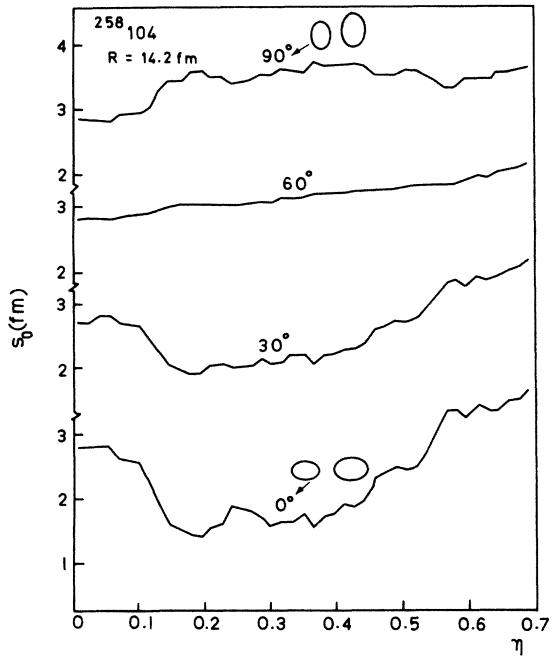

FIG. 9. The surface separation s_0 as a function of mass asymmetry η for $R=14.2$ fm and for different orientations $\theta_1=\theta_2=\theta$, for the compound system $^{258}104$.

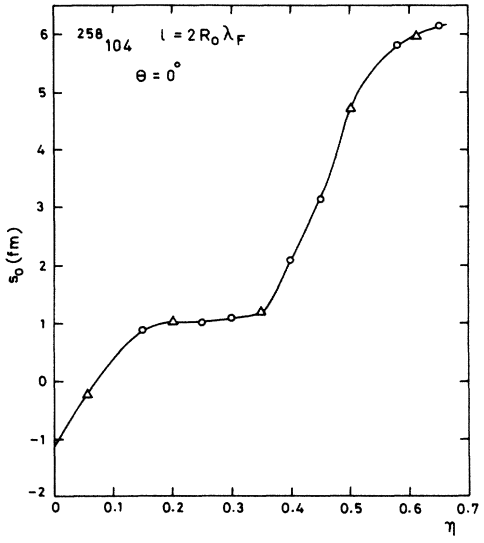

FIG. 11. The surface separation s_0 as a function of mass asymmetry η for the interaction region ($R<R_1+R_2,\theta=0°$), calculated for the length $\lambda_F(\eta)$ of the compound system $^{258}104$.

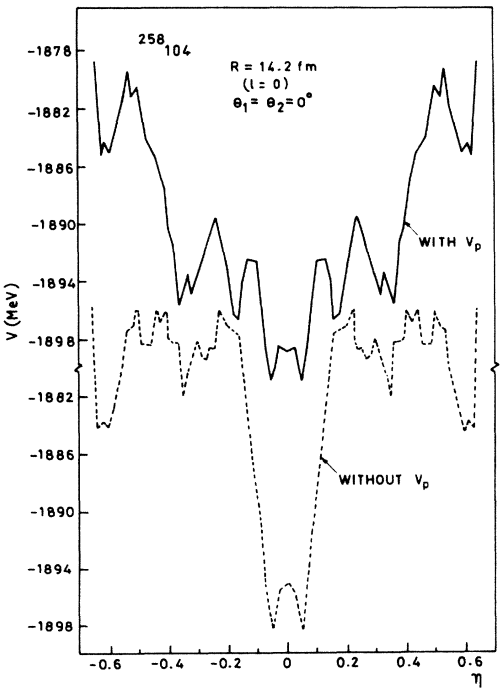

FIG. 10. The fragmentation potential V as a function of mass asymmetry η at $R=14.2$ fm, $\theta=0°$, and $l=0$ for the compound system $^{258}104$. The solid and the dashed lines give, respectively, the potential with and without V_p in it.

independent of η, for the spherical nuclei ($\beta_1=\beta_2=1$). However, it becomes strongly attractive for the deformed colliding nuclei and this attraction is shown to increase as the deformation increases [see the solid curve for $\theta=0°$ in Fig. 8(a); for deformations of the two colliding partners, see Fig. 8(b)]. We further notice in Fig. 8(a) that as θ increases the proximity potential $V_p(\eta)$ rapidly decreases and becomes almost zero at $\theta=90°$. This result is a simple manifestation of the fact that as the orientations θ of deformed nuclei increase, the surface separation s_0 increases (and hence, in view of our result for $R=15$ fm, the proximity potential decreases), as is shown in Fig. 9. As we go to $R<14.2$ fm, the proximity potential for spherical nuclei becomes a couple of tens of MeV more attractive, but then for deformed nuclei it is larger than or at least of the order of -100 MeV, which is rather an unrealistic value if V_p is simply an additional attraction due

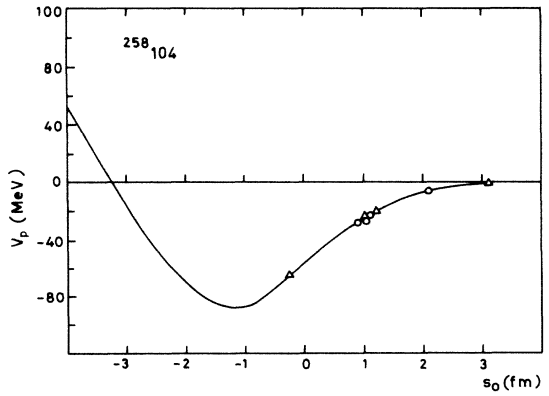

FIG. 12. The proximity potential (triangles and open circles) as a function of the surface separation $s_0(\eta)$ determined in Fig. 11. The calculations are made for $\eta\leq 0.5$ only and the solid line is drawn as a guide to the eye.

to the close proximity of the colliding surfaces. In another calculation, Saroha *et al.*[31] have shown that the role of the proximity potential is negligibly small for spherical and nearly spherical nuclei even for their touching configuration. Hence, this calculation along with that of Ref. 31 allows us to conclude that the proximity potential contributes significantly only for deformed colliding nuclei, and this contribution decreases gradually as the orientations of the colliding nuclei increase.

In order to see the role of the proximity effect in the fragmentation potential, we have shown in Fig. 10 (solid line) the fragmentation potential $V(\eta)$ for $^{258}104$, calculated by using Eq. (3), for $R=14.2$ fm, $\theta=0°$, and $l=0$. For comparison, the fragmentation potential for $V_p=0$ is also shown in Fig. 10 (dashed line). We notice that whereas the locations of the potential energy minima with respect to η remain almost unchanged, their relative excitation energies are strongly affected. Specifically, inclusion of the proximity term in the fragmentation potential makes the excitation energies of the target-projectile combinations, corresponding to the potential minima, increase with the increase of their mass asymmetry. This is an important result, as is discussed in the main text of this paper, as well as in II.

For the interaction region ($R<R_1+R_2$), we first obtain the variation of the surface separation s_0 as a function of mass asymmetry η by using Eq. (A7) for $\lambda=\lambda_F(\eta)$ taken from Fig. 4. This is shown in Fig. 11 and is relevant for $\eta\leq 0.5$ only, since no necked shapes appear after $\eta=0.5$ (see Fig. 2). The corresponding proximity potential V_p, calculated by using Eq. (5), is shown as triangles and open circles in Fig. 12. It is interesting to find that these calculated points give rise to a standard form of the proximity potential which is shown here by the solid line. (The calculated points could also be joined to give the modified form of the proximity potential of Blocki and Swiatecki,[32] but we have drawn here only the form used.) Apparently, our use of Eq. (A7) for determining s_0 in the case of necked systems formed by any two colliding nuclei and then using it in Eq. (5) for calculating the proximity potential seems justified. The fragmentation potential for the length $\lambda_F(\eta)$, with V_p included in it, is already shown in Fig. 5 and is found to give results similar to those for $R\geq R_1+R_2$ (see the main text).

---

*Permanent address: Physics Department, Panjab University, Chandigarh-160014, India.

[1]A. Săndulescu, R. K. Gupta, W. Scheid, and W. Greiner, Phys. Lett. **60B**, 225 (1976).

[2]R. K. Gupta, A. Săndulescu, and W. Greiner, Phys. Lett. **67B**, 257 (1977).

[3]R. Aroumougame and R. K. Gupta, J. Phys. G **6**, L155 (1980).

[4]R. K. Gupta, R. Aroumougame, and N. Malhotra, Lett. Nuovo Cimento **32**, 137 (1981).

[5]W. J. Swiatecki, Nucl. Phys. **A376**, 275 (1982).

[6]Yu. Ts. Oganessian, A. G. Demin, A. S. Iljinov, S. P. Tretyakova, A. A. Pelve, Yu. E. Penionzhkevich, M. P. Ivanonv, and Yu. P. Tretyakov, Nucl. Phys. **A239**, 157 (1975); Yu. Ts. Oganessian and Yu. E. Penionzhkevich, Joint Institute for Nuclear Research (Dubna) Report E7-9187, 1975.

[7]G. M. Ter-akopyan, A. S. Iljinov, Yu. Ts. Oganessian, A. O. Chepigin, B. V. Shilov, and G. N. Flerov, Nucl. Phys. **A255**, 509 (1975).

[8]R. Bock, Y. T. Chen, M. Dakowski, A. Gobbi, E. Grosse, A. Olmi, H. Sann, D. Schwalm, U. Lynen, W. Müller, S. Bjørnholm, E. Esbensen, W. Wolfi, and E. Morenzoni, Nucl. Phys. **A388**, 334 (1982).

[9]R. Aroumougame, N. Malhotra, and R. K. Gupta (unpublished).

[10]J. A. Maruhn and W. Greiner, Phys. Rev. Lett. **35**, 548 (1974).

[11]R. K. Gupta, W. Scheid, and W. Greiner, Phys. Rev. Lett. **35**, 353 (1975).

[12]J. Maruhn and W. Greiner, Z. Phys. **251**, 431 (1972).

[13]V. M. Strutinsky, Nucl. Phys. **A95**, 420 (1967); **A122**, 1 (1968).

[14]W. D. Myers and W. J. Swiatecki, Ark. Fiz. **36**, 343 (1967).

[15]W. Scheid and W. Greiner, Z. Phys. **226**, 364 (1969).

[16]P. A. Seeger, CERN Report 70-30, Vol. I, 1970, p. 217; Nucl. Phys. **A238**, 491 (1975).

[17]M. Münchow, D. Hahn, and W. Scheid, Nucl. Phys. **A388**, 381 (1982).

[18]M. J. Rhoades-Brown, V. E. Oberacker, M. Seiwert, and W. Greiner, Z. Phys. A **310**, 287 (1983).

[19]C. Y. Wong, Phys. Rev. Lett. **31**, 766 (1973).

[20]J. O. Hirschfelder, C. F. Curtiss, and R. B. Bird, *Molecular Theory of Gases and Liquids* (Wiley, New York, 1954), Chap. 12, pp. 846, 906–910.

[21]J. R. Nix, Ph.D. thesis, University of California, 1964.

[22]A. G. Webster, *The Dynamics of Particles and of Rigid Elastic and Fluid Bodies,* 3rd ed. (Hafner, New York, 1949), pp. 421–425.

[23]J. Blocki, J. Randrup, W. J. Swiatecki, and C. F. Tsang, Ann. Phys. (N. Y.) **105**, 427 (1977).

[24]M. Seiwert, W. Greiner, V. Oberacker, and M. J. Rhoades-Brown, Phys. Rev. C **29**, 477 (1984).

[25]N. Malhotra and R. K. Gupta, Phys. Rev. C **31**, 1179 (1985).

[26]J. Randrup and J. S. Vaagen, Phys. Lett. **77B**, 170 (1978).

[27]A. J. Baltz and B. F. Bayman, Phys. Rev. C **26**, 1969 (1982).

[28]H. H. Gutbrod, W. G. Winn, and M. Blann, Nucl. Phys. **A213**, 267 (1973).

[29]J. A. Maruhn, W. Greiner, and W. Scheid, *Heavy Ion Collisions,* edited by R. Bock (North-Holland, Amsterdam, 1980), Vol. 2, Chap. 6.

[30]H. Tricoire, H. Flocard, and D. Vautherin, Phys. Lett. **100B**, 106 (1981).

[31]D. R. Saroha, N. Malhotra, and R. K. Gupta, J. Phys. G **11**, L27 (1985).

[32]J. Blocki and W. J. Swiatecki, Ann. Phys. (N.Y.) **132**, 53 (1981).